

# Molecular simulation of host–guest inclusion compounds: an approach to the lactodendrimers case

S. Pricl\*, M. Fermeglia

Department of Chemical, Environmental and Raw Materials Engineering, University of Trieste, Piazzale Europa 1, 34127 Trieste, Italy

This work is dedicated to the memory of Iain C. M. Dea

Received 7 February 2000; revised 24 April 2000; accepted 5 May 2000

## Abstract

Molecular dynamics is applied to characterize the isolated structures of the first two generations of lactodendrimers as well as their possible inclusion complexes with four well-known molecular drugs. The results seem to indicate that the first generation can easily include small drugs, whereas a larger guest such as the second generation is necessary to fully and stably engulf bulkier compounds such as testosterone and cortisone. © 2001 Elsevier Science Ltd. All rights reserved.

**Keywords:** Lactodendrimers; Poly(propylene imine)dendrimers; Host–guest inclusion compounds; Molecular modeling; Molecular dynamics simulations

## 1. Introduction

As a new class of materials, dendrimers (or starburst polymers) have recently awakened great interest in the scientific community. Despite the substantial difficulties encountered in their synthesis, a wide range of these substances have been produced and, although only in part, characterized (Freché & Hawker, 1996; Matthews, Shipway & Stoddart, 1998; Newkome, Moorefield & Vögtle, 1996; Tomalia, Naylor & Goddard, 1990).

Starburst dendrimers possess three major architectural components: an initiator core, an interior and an exterior (see Fig. 1). By definition or construction, these three components are interdependent and reflect a unique molecular genealogy. As we progress from the initiator core to an advanced dendrimer stage (or *generation*), this molecular genealogy manifests itself in a variety of ways. Thus, beginning with the core, molecular details are sequentially transcribed and stored to produce interior and, ultimately, exterior features that are characteristic of that dendrimer family. In this fashion, interior features such as size, chemical composition, flexibility and topology are developed and manifested as stored molecular information.

The interior of a dendrimer consists of a scaffolding upon which surface properties such as shape, reactivity, stoichiometry, congestion, special kinetic features, flexibility and

fractal character can be generated and controlled. These surface features may reflect in several interesting attributes, such as divergent recognition (Cram, 1988) and exo-reception properties (Lehn, 1988), which find an analogy in biological processes like, for instance, antibody–antigen recognition (Amit, Mariuzza, Phillips & Poljak, 1986) and protein–protein interactions (Lewis & Rees, 1985).

These are by no means the only fascinating aspects of these molecules. In fact, many other potential applications spring from their unusual architecture, which includes nanoscale catalysis and reaction vessels (Bhryappa, Young, Moore & Suslick, 1996; Brunner, 1995), micelle mimics, magnetic imaging agents (Wiener et al., 1994), immuno-diagnostics, agents for controlled drug delivery (Singh, Moll, Lin & Ferzli, 1996; Tam, 1995), chemical sensors, information-processing materials, high-performance polymers, adhesives and coatings, separation media and molecular antennae for adsorbing light energy and funneling it to a central core (as occurs in photosynthetic systems) (Tomalia et al., 1990).

Among the plethora of possible dendrimers, poly(propylene imine) dendrimers have been synthesized on a relatively large scale and characterized—both experimentally and by molecular simulations—only in recent years (Blasizza, Fermeglia & Pricl, 2000; de Brabander & Meijer, 1993; de Brabander et al., 1996; de Brabander, Brackman, Froehling, Scherrenberg & Put, 1997; Jansen, Meijer & de Brabander, 1995; Stavelmans, van Hest, Jansen, van Boxtel, de Brabander & Meijer, 1996). The synthesis of a poly(propylene

\* Corresponding author. Tel: +39-40-6763750; fax: +39-40-569823.

E-mail address: sabrinap@dicamp.univ.trieste.it (S. Pricl).

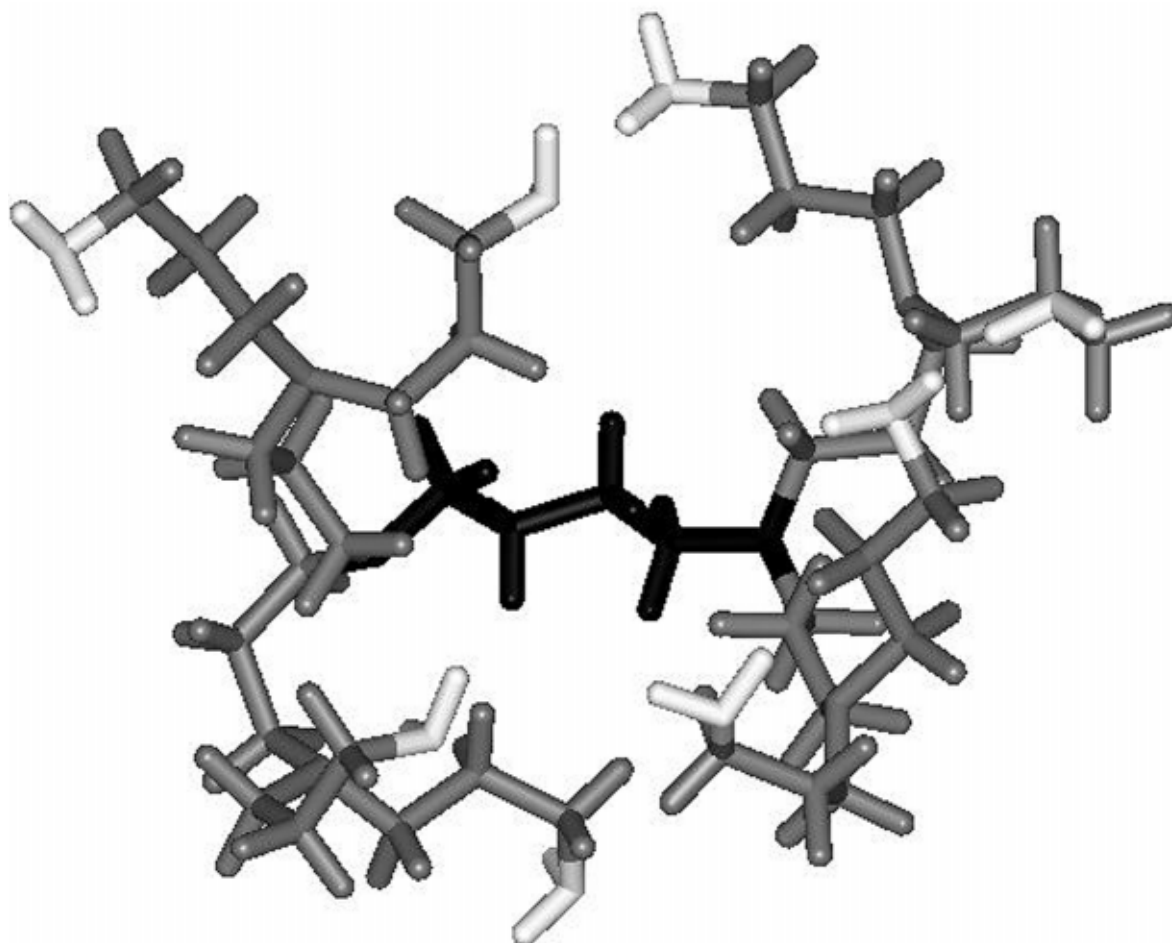


Fig. 1. Major architectural components of a dendritic molecule. Black: initiator core; gray: interior; white: exterior.

imine) dendrimer usually starts with a 1,4-diaminobutane core (DAB), to which four molecules of acrylonitrile are added in a fourfold Michael addition. The resulting tetranitrile of the first generation is then hydrogenated using a transition metal catalyst, which gives the tetra-amine of the first generation. The cycle of Michael additions and hydrogenations is then repeated to obtain higher generations.

The potential applications of the poly(propylene imine) dendrimers are generally based on one or more of the following characteristics:

- regular size and shape;
- large number of readily accessible end groups, either nitrile or amine;
- possibility of end group modification in order to tailor properties such as solubility, reactivity, toxicity, stability and glass transition temperature;
- polyelectrolyte character; and
- possibility of encapsulating guest molecules.

Even more recently, the synthesis of a series of carbohydrate-coated poly(propylene imine) dendrimers (hereafter

referred to as lactodendrimers, LDs) has been reported in the literature (Ashton et al., 1997), and subjected to an extensive hydrodynamic investigation (Pavlov et al., 1999). Since, however, their full application potentials (particularly in materials science and engineering) will not be realized before the understanding of their physical properties is considerably more advanced, in this work we report the first results obtained from an investigation of the structural details of the first two generations of LDs. In order to verify the validity of the data obtained on isolated structures, we report also the comparison of the information gained on the same structures in an aqueous environment with the available experimental data (Pavlov et al., 1999). Finally, we show and discuss the results obtained from an investigation of the interaction between LDs and four molecules of pharmaceutical interest. The relevance of this information is twofold. First, from it we can assess whether these first two LD generations can be considered as potential guest compounds and, second, we can verify if computer experiments can be considered as useful tools for characterizing host–guest systems comprising a large number of atoms and possessing rather complex molecular architectures.

## 2. Computational details

All simulations were run on a Silicon Graphics Origin 200 (microprocessor *MIPS RISC* 10000, 64 bit CPU, 128 MB RAM) and performed by using the commercial software *Cerius*<sup>2</sup> (v. 3.9) from Molecular Simulation Inc. (for both molecular mechanics (MM) and molecular dynamics (MD) simulations) and in-house developed codes (stand-alone and add-on to the commercial package).

The generation of accurate LD model structures was conducted as follows. For each dendrimer generation, the molecule was built and its geometry optimized via energy minimization using the COMPASS force field (Sun, 1994, 1995, 1998). The COMPASS FF is an augmented version of the CFF series of force fields and is the first ab initio force field that has been parameterized and validated using condensed-phase properties in addition to various ab initio and empirical data for molecules in isolation. The bond terms of the COMPASS FF potential energy function include a quartic polynomial both for bond stretching and angle bending, a three-term Fourier expansion for torsions and a Wilson out-of-plane coordinate term. Six crossterms up through the 3rd order are present to account for coupling between the intramolecular coordinates. The final two nonbonded terms represent the intermolecular electrostatic energy and the van der Waals interactions, respectively; the latter employs an inverse 9th power term for the repulsive part rather than the more customary 12th power term. The molecules were modeled to have a total charge equal to zero, and the distribution of the partial charge within each molecule was determined by the charge equilibration method of Rappé and Goddard (1991). Energy was minimized by up to 5000 Newton–Raphson iterations. Following this procedure, the root-mean-squares (rms) atomic derivatives in the low energy regions were smaller than 0.05 kcal/(mol Å). Long-range nonbonded interactions were treated by applying suitable cutoff distances, and to avoid the discontinuities caused by direct cutoffs, the cubic spline switching method was used. van der Waals distances and energy parameters for nonbonded interactions between heteronuclear atoms were obtained by the 6th-power combination rule proposed by Waldman and Hagler (1993).

The four drug molecules considered for the host–guest interaction studies were acetyl salicylic acid, dopamine, testosterone and cortisone. Their molecular models were built according to the procedure used for the LDs described above.

The calculations of molecular surface areas and volumes were performed using a modified version of the so-called Connolly dot surfaces algorithm (Connolly, 1983, 1985). Accordingly, a probe sphere of a given radius  $p_r$ , representing a solvent molecule, is placed in the region of the atoms of the molecule at thousands of different positions. For each position in which the probe does not experience van der Waals overlap with the atoms of the molecule, points lying on the inward-facing surface of the probe sphere

become part of the molecule *solvent-accessible surface* ( $S_{AS}$ ). According to this procedure, the molecular surface generated consists of the van der Waals surface of the atoms which can be touched by a solvent-sized probe sphere (called the *contact surface*), connected by a network of concave and saddle surfaces (globally called *re-entrant surfaces*) that smoothes over crevices and pits between the atoms of the molecule. The sum of the contact and the re-entrant surfaces forms the so-called *molecular surface* (MS); this surface is the boundary of the molecular volume (MV) that the solvent probe is excluded from if it is not to overlap with the molecule atoms, which therefore is also called the *solvent-excluded volume*. Finally, performing the same procedure by setting the probe sphere radius equal to zero, the algorithm yields the *van der Waals surface* (WS).

The Connolly algorithm can be considered a good technique for calculating molecular surfaces, but the same procedure has been proved less accurate for the determination of molecular volumes. Indeed, it has been observed that the molecular volumes derived using algorithms based on van der Waals radii are generally 30% lower than the experimentally determined volumes for small molecules (Rellick & Bechtel, 1997). Therefore, for the calculation of all molecular areas and volumes, we employed a method based on semiempirical molecular orbital calculations. First, the electron density distribution of the molecule was determined using the AM1 algorithm as implemented in the MOPAC package present in *Cerius*<sup>2</sup>. Accordingly, we calculated the electron density of the molecule at each point of a grid covering the molecule, allowing the grid size and the space between grid points to be varied. Since the orientation of the molecule within the grid can also be varied, the errors that occur from using a grid of a specific spacing and size can be quantified. The electron density value for each point of the grid was then used to calculate the area and volume of each molecule as a function of the percentage of the total calculated electronic density, according to a calculation technique implemented in a Fortran routine developed in-house. In this way, no assumption was made about the value of the radii of individual atoms or groups of atoms.

The details of the isolated dendrimer structures and the relevant inclusion complexes at 298 K were obtained by performing MD simulations under isochoric/isothermal (NVT) conditions. Each molecular dynamics run was started by assigning an initial velocity for the atoms according to a Boltzmann distribution at  $2 \times T$ . Temperature was controlled via weak coupling to a temperature bath (Andersen, 1980), with coupling constant  $\tau_T = 0.01$  ps. The Newton molecular equations of motion were solved by the Verlet leapfrog algorithm (Verlet, 1967), using an integration step of 1 fs. Since the partial charges assigned by the charge equilibration method are dependent on structure geometry, they were updated regularly every 100 MD steps during the entire MD runs. For the structural study of the LDs in the aqueous environment, a LD molecule

was confined, together with 100 water molecules, in a cubic box with periodic boundary conditions (PBC). Each water molecule was modeled by a simple 3-point charge (SPC) model, which has been verified to satisfactorily describe the properties of bulk water at ordinary temperatures (Berendsen, Postma, Di Nola, van Gunsteren, & Haak, 1984). In order to minimize the artifact of periodicity, a cutoff distance was set equal to half the box length. The resultant structures were relaxed via MM, again using the COMPASS FF; in this case, the Ewald technique was employed in handling nonbonded interactions.

Each MD simulation consisted of a system equilibration phase, during which the equilibration process was followed by monitoring the behavior of both kinetic and potential energy, and a successive data collection phase. Almost in all cases, the energy components ceased to show a systematic drift and have started to oscillate about steady mean values around 50 ps. Accordingly, equilibration phases longer than 100 ps (i.e. 1 000 000 MD steps with time step = 1 fs) and data acquisition runs longer than 500 ps were judged not necessary to enhance data accuracy.

### 3. Results and discussion

#### 3.1. The lactodendrimers

Fig. 2(a) and (b) show the wire-frame structures of the first two generations of lactodendrimers obtained as a result of the first structural investigations performed with MD simulations under NVT conditions. The first generation of these LDs is somewhat amorphous in shape, but the second one is already nearly spherical. This transition to a spheroidal form can be quantified by the aspect ratio of the principal moments for various generations (see Table 1). The ratio of the largest to smallest principal moment ( $I_z/I_x$ ) decreases from 1.8 for generation 1 to 1.5 for generation 2. Accordingly, the high initiator core multiplicity ( $N_c = 4$ ), combined with the branch multiplicity ( $N_b = 2$ ), results in very compact, highly congested microdomains, which possess, at most, only small internal voids.

A quantitative analysis of the internal surface area and solvent filled volume can be made by resorting to the concept of solvent accessible surface ( $S_{AS}$ ), as determined by the modified Connolly algorithm. Indeed, if we consider for instance, the surface of an ideal, spherical macromolecule containing no internal voids, then a plot of  $\sqrt{S_{AS}}$  vs. the molecular probe radius  $p_r$  would be linear, with an intercept proportional to the radius  $R$  of the macromolecule. Fig. 3 shows the plot of  $\sqrt{S_{AS}}$  as a function of the probe radius  $p_r$  for the two generations of LD simulated. Indeed, for large values of  $p_r$ ,  $\sqrt{S_{AS}}$  becomes independent of  $p_r$  as expected, since the lactodendrimers are neither ideally spheroidal, nor devoid of internal spaces; nevertheless, for small probe radii, a deviation from linearity is observed, owing to the extra surface area associated with the interior regions of the molecule.

Table 1

Aspect ratio of the principal moments for the first two generations of LDs

Generation	$I_z/I_x$	$I_z/I_y$	$I_y/I_x$
1	1.79	1.13	1.58
2	1.53	1.05	1.45

A linear regression analysis of these data indicates both the amount of any internal surface area ( $A_{INT}$ ) and the size ( $R_{AINT}$ ) of the lactodendrimers (see Table 2). As we can see from this table, the fraction of internal surface  $A_{INT}$  ranges from approximately 14.7% for generation 1 to 20.5% for generation 2. This behavior is similar to that exhibited by the parent series of dendrimers, the poly(propylene imine) dendrimers, although, in this latter case, the increase in internal surface area was more marked in passing from first to second generation (i.e.  $A_{INT}$  ranged from 4.1 to 9%) (Blasizza et al., 2000). This result seems reasonable, since the conformational transition from an amorphous to a spheroidal shape is decidedly more marked for the parent dendrimers: in this case,  $I_z/I_x$  decreases from 2.2 to 1.1 in passing from generation 1 to generation 2 (Blasizza et al., 2000).

A measure of the volume associated with the internal cavities of the lactodendrimers can be achieved analyzing the behavior of the solvent excluded volume  $V_{SE}$ , again as a function of the probe radius  $p_r$ . If we consider Fig. 4, where we report  $V_{SE}^{1/3}$  vs.  $p_r$  for both dendrimer generations, we see that again a linear relationship is obtained for large probe radii but there is a limited deficit of volume for small  $p_r$  ( $V_{INT}$ ) (approximately 10% for both molecules, see Table 2), owing to the presence of small internal cavities and channels. Once again, this behavior is reminiscent of that shown by the parent starburst molecules (i.e.  $V_{INT}$  ranged from 8 to 12% for the corresponding first two generations), and of other dendrimer series as well (Tomalia et al., 1990).

Molecular modeling and molecular dynamics simulations were also used to estimate the size of both series of DAB dendrimers as a function of generation (see again Table 2). Four quantities were calculated from these experiments:

- $R_{AINT}$ , the radius determined from the linear regression fits of  $p_r$  vs.  $S_{AS}^{1/2}$ ;
- $R_{VINT}$ , the radius determined from the linear regression fits of  $p_r$  vs.  $V_{SE}^{1/3}$ ;
- $R_{gNVT}$ , the value of the radius of gyration, averaged over the entire set of trajectories during the collection phase of an NVT experiment (from 100 to 400 ps); and
- $R_{CKP}$ , the radius calculated from the maximal end-to-end distance between terminal groups, determined periodically and averaged over the entire set of NVT trajectories.

Generally speaking, there is very good agreement between all series of calculated values. These are, as expected, larger than those corresponding to the parent molecules, due to the bigger repeating units, but not much

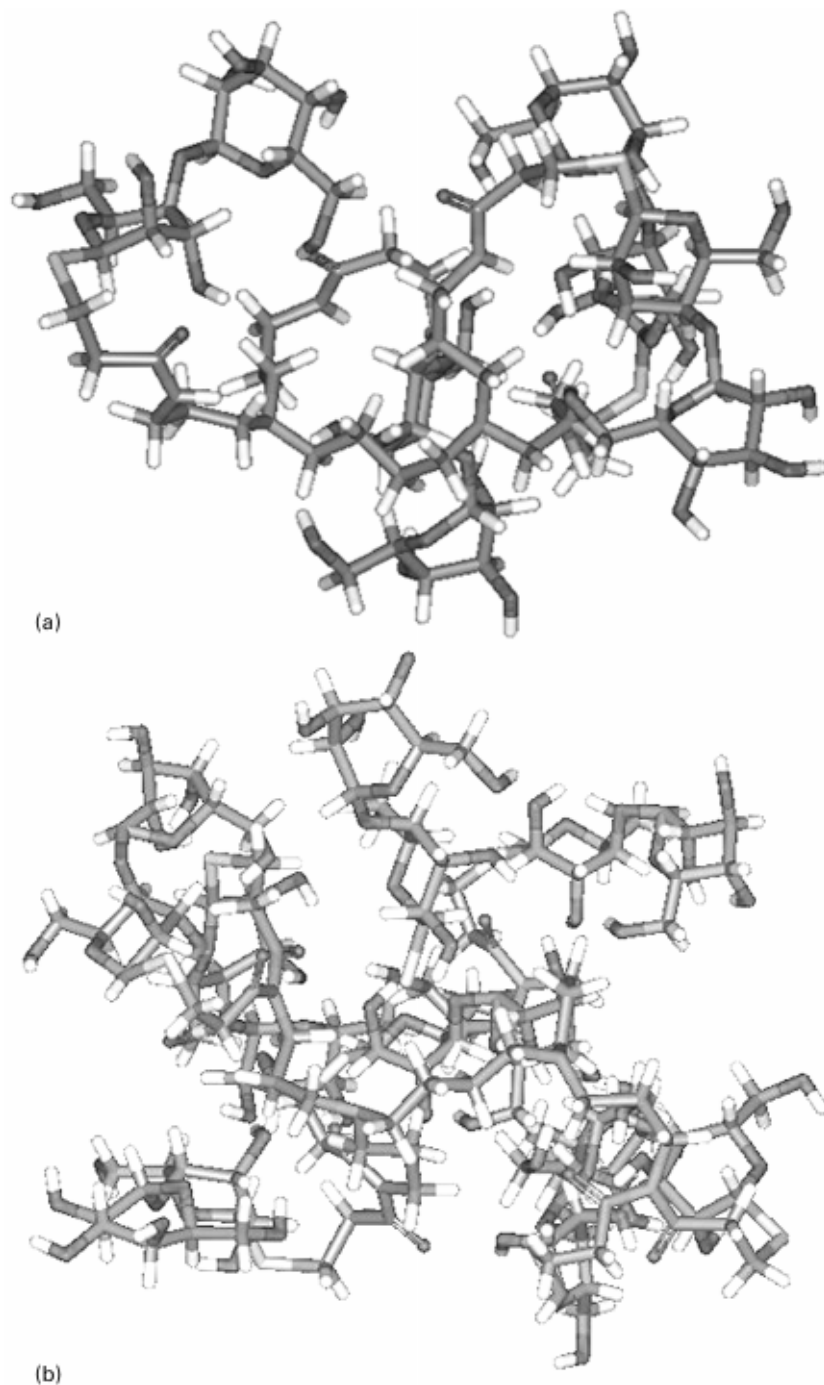


Fig. 2. Wire-frame representation of two equilibrated structures of LDs. (a) generation 1; (b) generation 2.

larger, since these dendrimers are, with respect to their parents, more compact.

Since no data were available on isolated molecules for comparison, in order to check the quality of these results we performed another set of MD simulations on these molecules in the presence of water, and Fig. 5 shows a sketch of the equilibrated simulation cell. Although no salts were included in the system, the values of the corresponding radius of gyration  $R_{g,WATER}$  obtained from these virtual

experiments for the first two generations are in very good agreement with the values obtained experimentally by Pavlov et al. (1999) (see Table 2). This seems to confirm the validity of the force field selection and the reliability of the applied simulation conditions.

### 3.2. The drugs

The validity of any molecular simulation rests on the

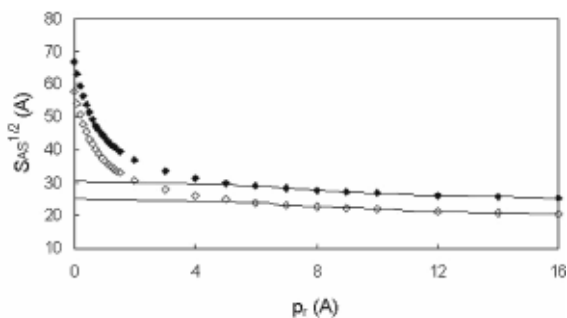


Fig. 3.  $\sqrt{S_{AS}}$  as a function of the probe radius  $p_r$  for the two generations of LD simulated. Open symbols: generation 1; filled symbols: generation 2.

suitability and accuracy of the equations used for the intermolecular potentials. Although the accuracy of a prediction may be estimated by considering the approximations and simplifications of the model and computational procedure, the final test lies in a comparison of theoretically predicted and experimentally measured properties. Table 3 shows the results of this comparison in terms of geometrical parameters for acetyl salicylic acid as an example. Utterly similar results were obtained for the remaining three active principles. From an inspection of this table, we can conclude that the agreement is more than satisfactory, and the resultant optimized structures of all the four drugs are given in Fig. 6(a)–(d).

### 3.3. The inclusion complexes

Having analyzed the structures of the isolated structures of the LD generations 1 and 2, and having ascertained that there exist internal voids that may be considered for the incorporation of small molecules without distinct geometry or functionality by a host–guest mechanism, we calculated the data relevant to the inclusion of the four well-known active drugs described in Section 3.2. Indeed, molecular modeling and molecular dynamics techniques may enable an efficient drug incorporation to be predicted; accordingly, the theoretical determination of the stabilization enthalpies of the complexes eventually formed may be of help in the selection of a promising coating or encapsulating material.

The energies involved in the interactions between the examined host–guest molecular couples are presented in Table 4 for LD generation 1 and for LD generation 2. These values were obtained by subtracting the average configuration energy (ACE) of the single components from the ACE of the complexes. In both cases, the nearly

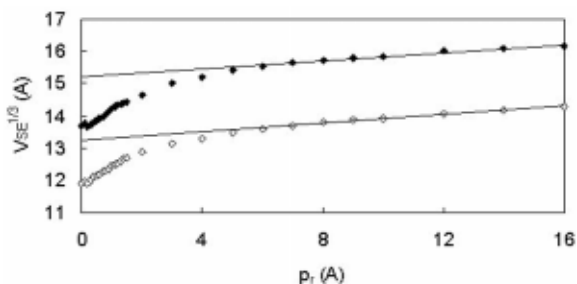


Fig. 4.  $V_{SE}^{1/3}$  as a function of the probe radius  $p_r$  for both dendrimer generations. Open symbol: generation 1; filled symbols: generation 2.

constant values of the main valence energy terms ( $E_{val} = E_{bond} + E_{angle} + E_{tors}$ ), coupled with the high calculated dipole moment of the active drug (see Table 5) is a first, clear indication that the host–guest inclusion takes place mainly on the basis of the dispersion and electrostatic interaction forces. Indeed, due to the chemical nature of the LDs, characterized by the presence of several oxygen and nitrogen atoms, many such interactions can occur between the polar drugs and the interior of the LDs, and a subsequent excellent nesting is the reason for the high stabilization enthalpies of the inclusion compounds.

For the LD generation 1, the inclusion complexes with acetyl salicylic acid, dopamine and testosterone show stabilization enthalpies that range from about  $-20.3$  kcal/mol up to about  $-26.1$  kcal/mol (see Table 4); a corresponding snapshot of the equilibrium configuration for each of these complexes is given in Fig. 7(a)–(c), respectively. As we may understand by examining Table 4, the major part of the complex stabilization is due to van der Waals forces. In particular, we split the contributions of this nature into intramolecular 1–4 interactions ( $E_{vdw}(1,4)$ ) and the sum of all other van der Waals increments ( $E_{vdw}$ ). Compared to the latter, the 1–4 van der Waals contributions are extraordinarily small for all compounds, indicating that the close neighborhood of the atoms does not change them electronically both in the host and in the guest compounds. Therefore, the inclusion mechanism seems to be similar to a lock and key principle without distinct conformational adaptation.

The second stabilization type worth mentioning is of an electrostatic nature. In Table 5 we present the calculated data for the dipole–dipole interactions between the LD generations 1 and 2 and the corresponding active drugs. The amount of these stabilizing forces depends upon the sum of the dipole moments of the isolated compounds as well as their orientation. In the case of LD generation 1, the

Table 2

Calculated internal dendrimer surface areas ( $A_{INT}$ ) and volumes ( $V_{INT}$ ) as well as molecular diameters obtained from the virtual experiments as a function of generation

Generation	$A_{INT}$ (%)	$R_{AINT}$ (Å)	$V_{INT}$ (%)	$R_{VINT}$ (Å)	$R_{CKP}$ (Å)	$R_{gNVT}$ (Å)	$R_{gWATER}$ (Å)
1	14.7	7.17	10.2	8.22	8.30	7.73	11.6
2	20.5	8.61	9.98	9.42	10.0	8.59	15.2

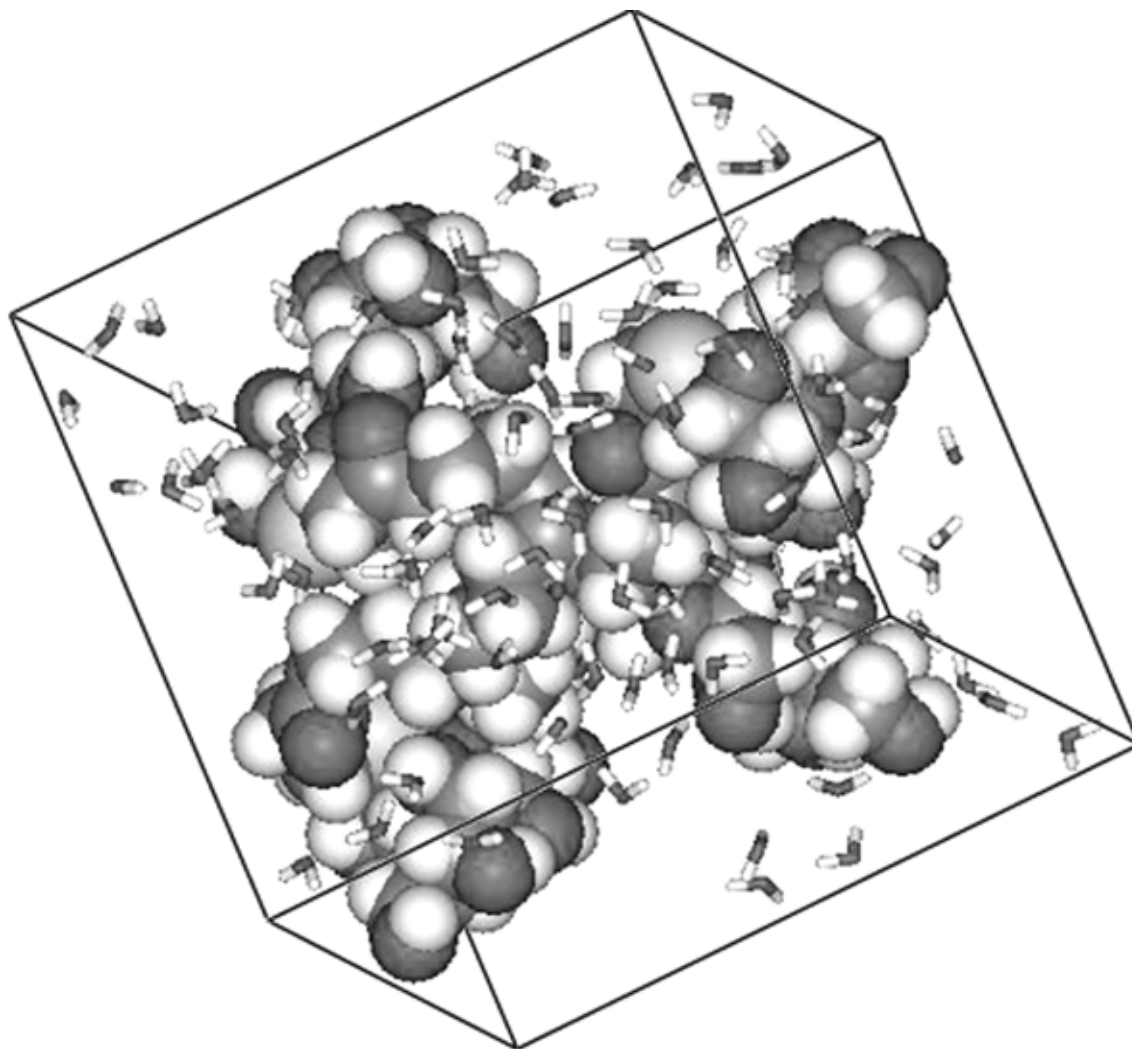


Fig. 5. Equilibrated simulation cell of LD generation 1 in water.

highest electrostatic stabilization enthalpy ( $E_{\text{coul}} = -4.82$  kcal/mol). corresponds to the inclusion complex of dopamine, since this molecule has both a high dipole moment  $\mu = 2.65$  debye) and the average angle of interaction with

Table 3  
Structural molecular parameters for acetyl salicylic acid: comparison between calculated and experimental data (in parenthesis)

Acetyl salicylic acid	Bond length (Å) and bond angle (°)
C–C aromatic	1.397 (1.399)
C–H aromatic	1.100 (1.101)
C=O	1.220 (1.214)
C–O	1.369 (1.364)
O–H	0.950 (0.956)
C–C	1.523 (1.520)
C–H aliphatic	1.099 (1.10)
C–C=O	125.1 (125.6)
H–C–H aliphatic (average)	108.5 (108.5)
C–O–H	108.2 (109.0)

the LD dipole moment of  $150^\circ$  is nearest to its optimum value (i.e.  $180^\circ$ ). At the other end of the series we found the LD (generation 1)/testosterone complex, whose electrostatic stabilization energy amounts to  $-1.00$  kcal/mol, due to the quite unfavorable angle of  $71^\circ$  between the host and the guest molecules.

The inclusion complex of LD generation 1 with cortisone deserves different comments. As appears evident from Table 4, aside from the electrostatic stabilizing contribution due to the favorable dipole–dipole interaction (see Table 5), all other interaction energy components are positive and, hence, destabilizing. In our opinion, the inner contact surface of the LD generation 1 molecule is the limiting factor for the development of an effective incorporation geometry and, therefore, for a strong stabilization in the case of the big cortisone molecule (see Fig. 7(d)).

If we now consider the energies involved in the interactions between the examined host–guest molecular couples for LD generation 2, we clearly spot a different situation, since all four inclusion compounds show high

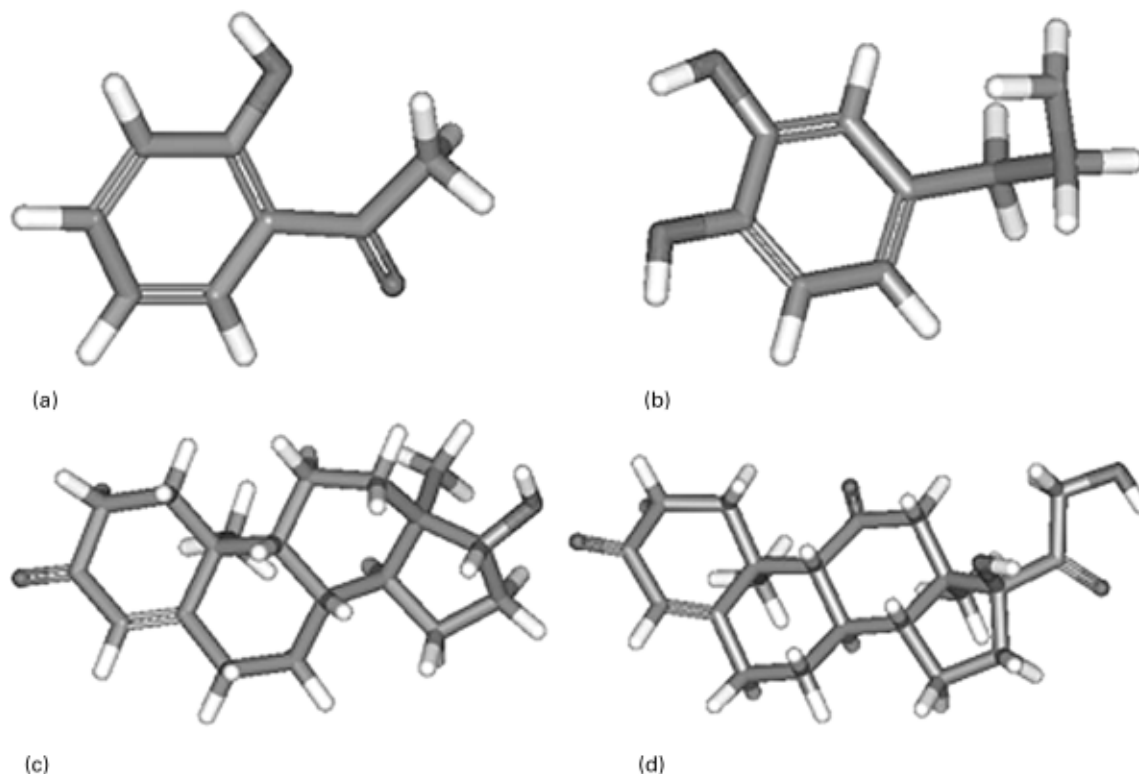


Fig. 6. Optimized molecular structures for the four drugs considered: (a) acetyl salicylic acid; (b) dopamine; (c) testosterone; and (d) cortisone.

overall host–guest stabilization enthalpies (see Table 4). Once again, the van der Waals and the electrostatic components of the energy are mainly responsible for the host–guest inclusion process. Nevertheless, the small first two active molecules, which are intimately adapted to the smaller, inner cavity of the LD first generation (see Table 4), show a decreasing intermolecular van der Waals stabilization contribution (from approximately  $-14$  kcal/

mol to about  $-10$  kcal/mol for both compounds) with increasing diameter of the host dendrimer (see Fig. 8(a) and (b)). On the other hand, in passing from LD generation 1 to generation 2, the bulky drugs are optimally incorporated into the inner cavity of the starburst host, as confirmed by the corresponding values of  $E_{vdw}$ . These inclusion complexes are further stabilized by highly negative electrostatic components, due in turn to the favorable

Table 4  
Energetic contributions of host–guest interactions

Energy component (kcal/mol)	Acetylic acid	Dopamine	Testosterone	Cortisone
<i>LD generation 1</i>				
$E_{bond}$	-2.41	-1.92	-2.25	0.968
$E_{angle}$	-1.78	-1.71	-2.27	0.116
$E_{tors}$	-2.56	-2.59	-2.69	1.09
$E_{vdw}(1,4)$	-0.20	-0.18	-0.24	0.0510
$E_{vdw}$	-14.2	-14.9	-11.8	0.737
$E_{coul}$	-2.54	-4.82	-1.00	-3.08
$\Delta H_f$	-23.7	-26.1	-20.3	-0.118
<i>LD generation 2</i>				
$E_{bond}$	-3.89	-2.33	-3.11	-3.92
$E_{angle}$	-1.96	-2.50	-2.89	-2.64
$E_{tors}$	-2.10	-1.56	-2.35	-2.81
$E_{vdw}(1,4)$	-0.20	-0.18	-0.29	-0.21
$E_{vdw}$	-10.9	-10.5	-15.4	-12.9
$E_{coul}$	-1.02	-1.50	-5.86	-6.18
$\Delta H_f$	-20.1	-18.6	-29.9	-28.7

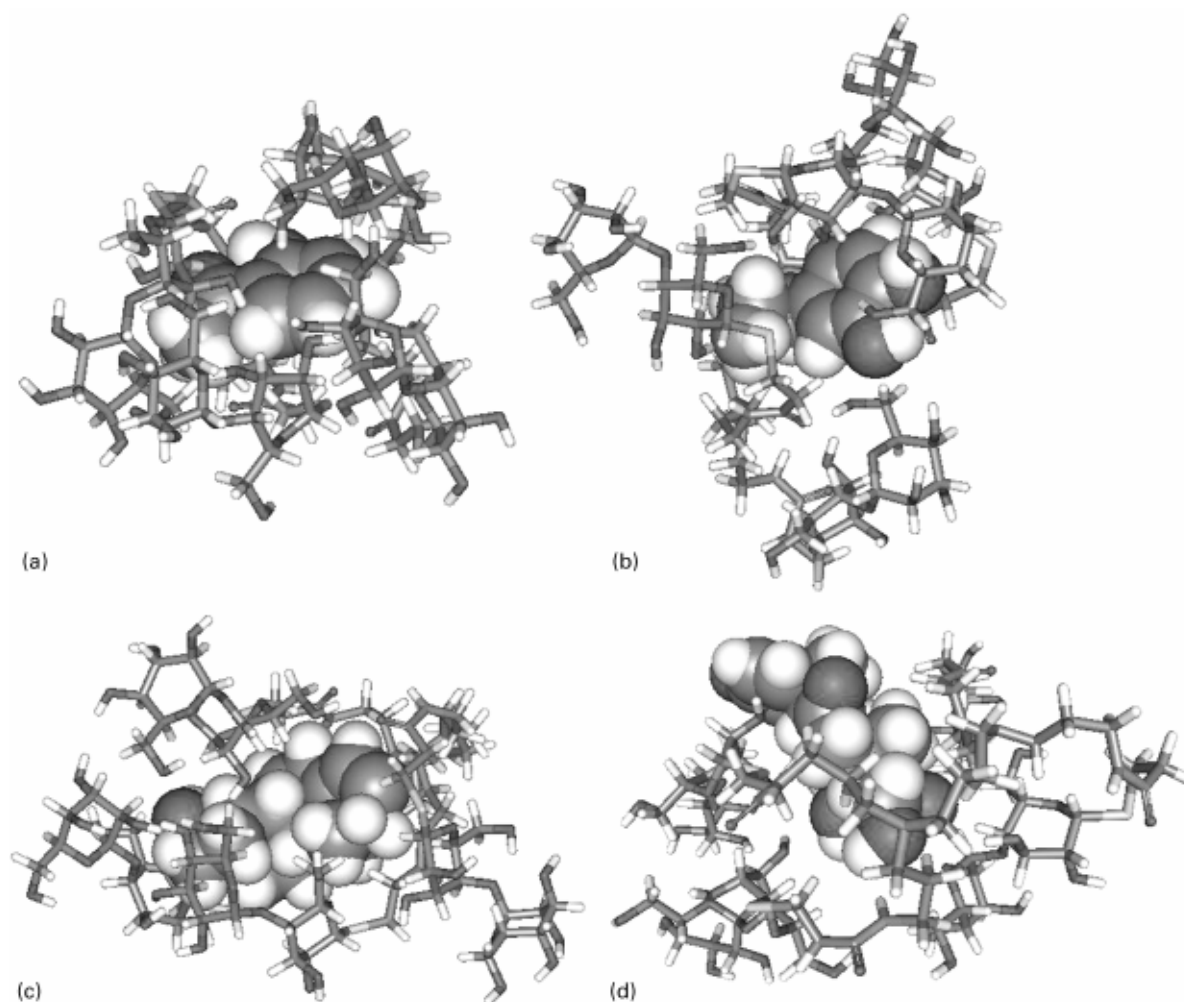


Fig. 7. Inclusion complexes of LD generation 1 with the four drugs considered: (a) with acetyl salicylic acid; (b) with dopamine; (c) with testosterone; and (d) with cortisone.

dipole–dipole interactions (see Table 5). Two relevant snapshots of the equilibrium inclusion complexes of testosterone and cortisone in LD generation 2 are given by Fig. 8(c) and (d), respectively.

#### 4. Conclusions

In this work we have shown how molecular modeling and molecular dynamics simulations can be used to investigate

the structural details of complex molecules, such as the first two generations of lactodendrimers, as well as for the interpretation of their eventual host–guest inclusion phenomena. The application of simple computer experiment techniques has allowed us to evaluate the amount of internal surface area and volume of the first two generations of these LDs and to calculate their isolated molecular dimensions. Since no experimental data were available for comparison, we also performed some simulations in an aqueous environment and found that our results, in terms of molecular dimensions, showed rather satisfactory agreement with the published information. Finally, we characterized the possible inclusion complexes of these promising starburst compounds with four model active drugs. The results obtained seem reasonable, indicating that generation 1 can easily include small drugs, whereas a larger guest such as generation 2 is necessary to fully and stably engulf bulkier compounds such as testosterone and cortisone. Further work is currently in progress to extend this information to higher LD generations and to host/guest inclusion complex formation in the presence of aqueous solvents.

Table 5  
Dipole–dipole interactions between the LDs and the four active drugs

Active drug	$\mu$ (debye)	Angle $_{\mu}$ (host/guest) (°)	
		Generation 1	Generation 2
Acetylic acid	4.02	106	102
Dopamine	2.65	150	116
Testosterone	2.63	71	123
Cortisone	4.46	128	157

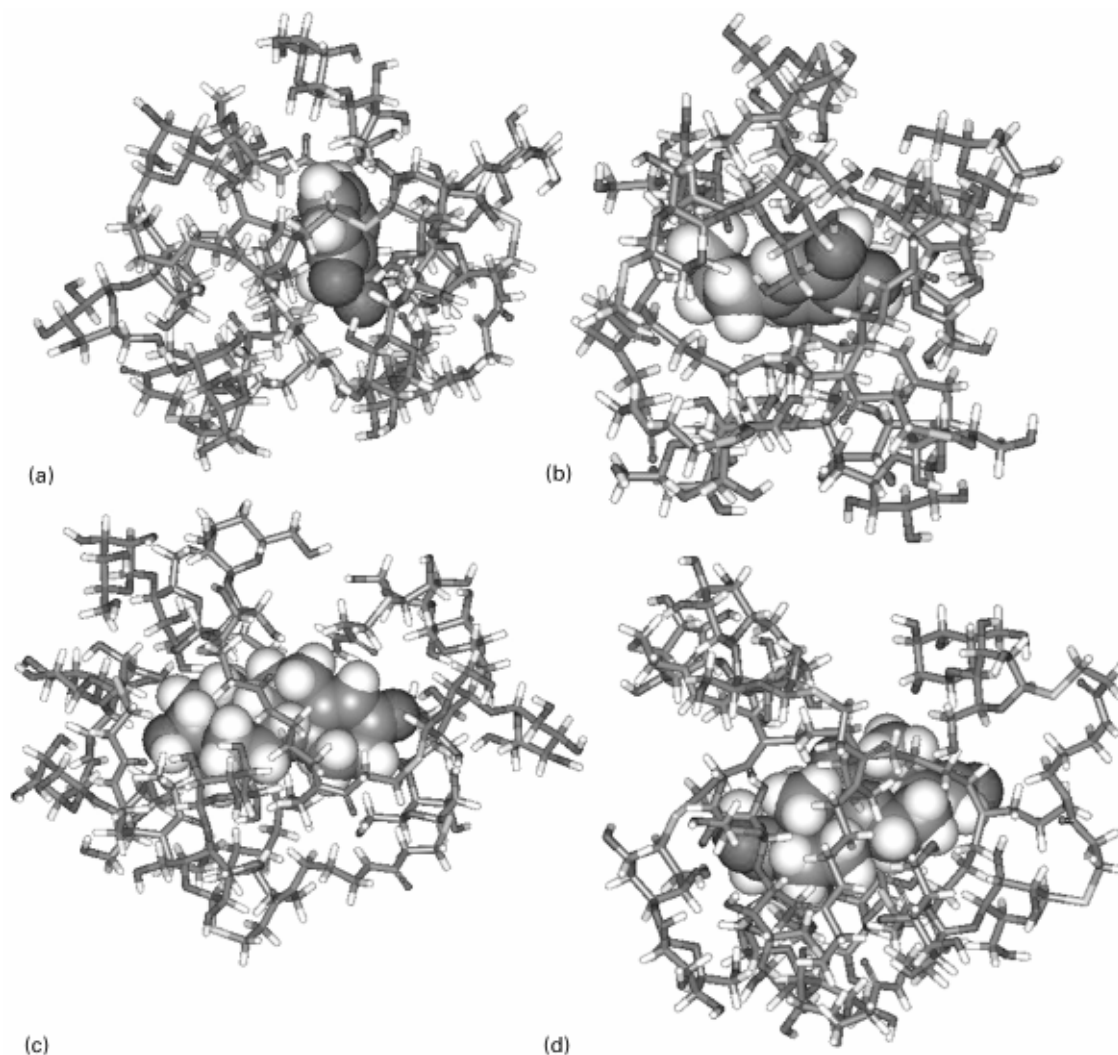


Fig. 8. Inclusion complexes of LD generation 2 with the four drugs considered: (a) with acetyl salicylic acid; (b) with dopamine; (c) with testosterone; and (d) with cortisone.

## Acknowledgements

The authors wish to thank the Italian Ministry for University and Scientific Research (MURST, Rome) and the University of Trieste (Special Grant for Scientific Research) for financial support.

## References

- Amit, A. G., Mariuzza, A. R., Phillips, S. E. V., & Poljak, R. J. (1986). Three-dimensional structure of an antigen–antibody complex at 2.8 Å resolution. *Science*, *233*, 747–753.
- Andersen, H. C. (1980). Molecular dynamics simulations at constant pressure and/or temperature. *Journal of Chemical Physics*, *72*, 2384–2393.
- Ashton, P. R., Boyd, S. E., Brown, C. J., Nepogodiev, S. A., Meijer, E. W., Peerlings, H. W. I., & Stoddart, J. F. (1997). Synthesis of glycodendrimers by modification of poly(propylene imine) dendrimers. *Chemistry European Journal*, *3*, 974–984.
- Berendsen, H. J. C., Postma, J. P. M., Di Nola, A., van Gunsteren, W. F., & Haak, J. R. (1984). Molecular dynamics with coupling to an external bath. *Journal of Chemical Physics*, *81*, 3684–3690.
- Bhyrappa, P., Young, J. K., Moore, J. S., & Suslick, K. S. (1996). Dendrimer–metalloporphyrins: synthesis and catalysis. *Journal of the American Chemical Society*, *118*, 5708–5711.
- Blasizza, E., Fermeglia, M., & Pricl, S. (2000). Dendrimers as functional materials. A molecular simulation study of poly(propylene imine) starburst molecules. *Molecular simulation*, (in press).
- de Brabander, E. M. M., & Meijer, E. W. (1993). Poly(propylene imine) dendrimers: large scale synthesis by heterogeneously catalyzed hydrogenations. *Angewandte Chemie International Edition in English*, *32*, 1308–1311.
- de Brabander, E. M. M., Brackman, J., Mure-Mak, M., de Man, H., Hogeweg, M., Keulen, J., Scherrenberg, R., Coussens, B., Mengerink, Y., & van der Wal, S. J. (1996). Poly(propylene imine) dendrimers: improved synthesis and characterization. *Macromolecular Symposia*, *102*, 9–17.
- de Brabander, E.M.M., Brackman, J., Froehling, P., Scherrenberg, R., Put, J. (1997). Structure, properties and applications of Astramol poly(propylene imine) dendrimers. In: *Proceedings of the American Chemical Society division of polymeric materials: science and engineering* (pp. 84,85). Fall meeting, Las Vegas, NE.
- Brunner, H. (1995). Dendrzymes: expanded ligands for enantioselective catalysis. *Journal of Organometallic Chemistry*, *500*, 39–46.
- Connolly, M. L. (1983). Solvent-accessible surfaces of proteins and nucleic acids. *Science*, *221*, 709–713.

- Connolly, M. L. (1985). Computation of molecular volume. *Journal of the American Chemical Society*, *107*, 1118–1124.
- Cram, D. M. (1988). The design of molecular hosts, guests and their complexes. *Angewandte Chemie International Edition in English*, *27*, 1009–1020.
- Fréchet, J. M. J., & Hawker, C. J. (1996). Synthesis and properties of dendrimers and hyperbranched polymers. In S. L. Aggarwal & S. Russo, *Comprehensive Polymer Science* (pp. 140–201). Oxford: Elsevier.
- Jansen, J. F. G. A., Meijer, E. W., & de Brabander, E. M. M. (1995). The dendritic box: shape-selective liberation of encapsulated guests. *Journal of the American Chemical Society*, *117*, 4417–4418.
- Lehn, J. M. (1988). Supramolecular chemistry—scope and perspectives. Molecules, supermolecules and molecular devices. *Angewandte Chemie International Edition in English*, *27*, 89–112.
- Lewis, M., & Rees, D. C. (1985). Fractal surfaces of proteins. *Science*, *230*, 1163–1165.
- Matthews, O. A., Shipway, A. N., & Stoddart, J. F. (1998). *Progress in Polymer Science*, *23*, 1–56.
- Newkome, G. R., Moorefield, C. N., & Vögtle, F. (1996). *Dendritic molecules: concepts, syntheses, perspectives*, Weinheim: VCH Verlagsgesellschaft.
- Pavlov, G. M., Korneeva, E. V., Jumel, K., Harding, S. E., Meijer, E. W., Peerlings, H. W. I., Fraser-Stoddart, J., & Nepogodiev, S. A. (1999). Hydrodynamic properties of carbohydrate-coated dendrimers. *Carbohydrate Polymers*, *38*, 195–202.
- Rappé, A. K., & Goddard III, W. A. (1991). Charge equilibration for molecular dynamics simulations. *Journal of Chemical Physics*, *95*, 3358–3363.
- Rellick, L. M., & Becktel, W. J. (1997). Comparison of van der Waals and semiempirical calculations of the molecular volumes of small molecules and proteins. *Biopolymers*, *42*, 191–202.
- Singh, P., Moll III, F., Lin, S. H., & Ferzli, C. (1996). Random detection of antigens with antibodies immobilized on soluble submicron particles. *Clinical Chemistry*, *42*, 1567–1569.
- Stavelmans, S., van Hest, J. C. M., Jansen, J. F. G. A., van Boxtel, D. A. F. J., de Brabander, E. M. M., & Meijer, E. W. (1996). Synthesis, characterization and guest–host properties of inverted unimolecular dendritic micelles. *Journal of the American Chemical Society*, *118*, 7398–7399.
- Sun, H. (1994). Force field for computation of conformational energies, structures, and vibrational frequencies of aromatic polyesters. *Journal of Computational Chemistry*, *15*, 752–768.
- Sun, H. (1995). Ab initio calculations and force field development for computer simulation of polysilanes. *Macromolecules*, *28*, 701–712.
- Sun, H. (1998). COMPASS: an ab initio force field optimized for condensed-phase applications—overview with details on alkane and benzene compounds. *Journal of Physical Chemistry B*, *102*, 7338–7364.
- Tam, J. P. (1995). Synthesis and applications of branched peptides in immunological methods and vaccines. *Peptides*, *155*, 455–500.
- Tomalia, D. A., Naylor, A. M., & Goddard III, W. A. (1990). Starburst dendrimers: molecular-level control of size, shape, surface chemistry, topology and flexibility from atoms to macroscopic matter. *Angewandte Chemie International Edition in English*, *29*, 138–175.
- Verlet, L. (1967). Computer experiments on classical fluids. I. Thermodynamical properties of Lennard-Jones molecules. *Physical Reviews*, *159*, 98–103.
- Waldman, M., & Hagler, A. T. (1993). New combining rules for rare gas van der Waals parameters. *Journal of Computational Chemistry*, *14*, 1077–1084.
- Wiener, E. C., Brechbiel, M. W., Brothers, H., Magnin, R. L., Gansow, O. A., Tomalia, D. A., & Lauterbur, P. C. (1994). Dendrimer-based metal chelates: a new class of magnetic resonance imaging contrast agents. *Magnetic Resonance in Medicine*, *31*, 1–8.